Sensors & Actuators: B. Chemical 290 (2019) 41–46

Contents lists available at ScienceDirect

Sensors and Actuators B: Chemical

journal homepage: www.elsevier.com/locate/snb

Fast detection of mycoplasma pneumoniae by interaction of tetramolecular G-quadruplex with graphene oxide

Juanjuan Li[a], Jie Wu[b], Zhengqing He[a], Hua Pei[a], Qianfeng Xia[a], Qiang Wu[a,*], Huangxian Ju[b,*]

[a] Laboratory of Tropical Biomedicine and Biotechnology, School of Tropical Medicine and Laboratory Medicine, Hainan Medical University, Haikou, 571199, China
[b] State Key Laboratory of Analytical Chemistry for Life Science, School of Chemistry and Chemical Engineering, Nanjing University, Nanjing, 210023, China

ARTICLE INFO

Keywords:
Biosensor
G-quadruplex
Fluorescence quenching
Point-of-care testing
DNA
Mycoplasma pneumoniae

ABSTRACT

Fast and sensitive detection of mycoplasma pneumoniae (MP) is quite momentous in early diagnosis of respiratory infections. Herein, we present a new biosensing platform for MP based on the interaction of a designed parallel-stranded tetrapod G-quadruplex (TP-G4) with graphene oxide. The G-quadruplex is formed with four fluorescent dye labeled ssDNA molecules, which is demonstrated with gel electrophoresis, CD spectra and fluorescence spectra. The interaction induces the adsorption of TP-G4 on graphene oxide, which leads to the fluorescence quenching of the dye. Upon the recognition of the adsorbed ends to target MP, the TP-G4 can be released from graphene oxide surface, producing a "signal-on" fluorescence biosensor for MP. The designed biosensing strategy shows a detection limit of 3.96 nM and an analytical time of 10 min. The facile and fast operation process and acceptable sensitivity meet the demands of early point-of-care testing of mycoplasma pneumoniae, showing its promising application in clinic diagnosis.

1. Introduction

Mycoplasma pneumoniae (MP), as the etiological agent of primary atypical pneumonia, can induce both the upper and the lower respiratory infections, and often occurs both endemically and epidemically worldwide in children and adults [1,2]. It accounts for as many as 20–40% of all cases of community-acquired pneumonia [3]. Although the majority of MP infections are mild, 25% of patients experience several complex extrapulmonary complications, including skin rashes [4], hemolytic anemia, pericarditis, prolonged joint pain, and severe neurological diseases [5], and there is still about 5%–10% of cases in high mortality. As a result, early detection of MP is of prime importance for clinical diagnostics.

Since the clinical manifestations of MP infection are often similar to those of other atypical pathogens [6], it is difficult to discern them from other causes of pneumonia through symptoms or chest X-ray, therefore, the diagnosis of MP infection hinges mainly on diagnostic laboratory tests. At present, the traditional laboratory diagnostic assays roughly include culture, serological and polymerase chain reaction (PCR) analysis [7]. The culture assays have a relatively low sensitivity, and the culture of a throat swab or sputum specimens is laborious, requiring specialized and expensive growth mediators, and taking more than one week of treatment. The serological analysis uses antibody as the biomarker, which lacks both the sensitivity to the onset of illness and the standardized kits. The most convincing evidence of serological test for MP is both IgM and IgG in the paired specimens collected at least 2–3 weeks apart, which is generally too slow for actual use [8]. PCR technique possesses high sensitivity and specificity, but requires skilled operators, expensive instruments and complex sample pretreatments, which is impossible to be widely used for early point-of-care testing of MP [6,9]. Therefore, it is particularly vital to develop an early, rapid and highly specific method for the diagnosis of MP infection to improve the cure rate, reduce the antimicrobial drug abuse, relieve the pain and alleviate the financial burden of patients. This work designed a convenient biosensing platform for MP based on the interaction of a parallel-stranded tetrapod G-quadruplex (TP-G4) with graphene oxide.

G-quadruplex, formed by the stacks of G-quartets bound together by four Hoogsteen-paired guanines [10,11], has been drawn considerable attention recently, and known to be stabilized in virtue of the monovalent cations, especially the potassium ions [12,13], holding between the G-quartets in the central cavity, to form an intermolecular structure [14–16]. These structures can be easily distinguished from other non-G-tetrahedral structures by nuclear magnetic resonance (NMR) and circular dichroism (CD) spectra, and have been demonstrated a potentially high stability [17], which renders them suitable for applications in biosensors. Therefore, several G-quadruplex based biosensors have been developed for the detection of various analytes, including metals [18,19], biomolecules [20] and other metabolites [21]. Although G-

* Corresponding authors.
E-mail addresses: wuqiang001001@aliyun.com (Q. Wu), hxju@nju.edu.cn (H. Ju).

https://doi.org/10.1016/j.snb.2019.03.103
Received 20 January 2019; Received in revised form 21 March 2019; Accepted 24 March 2019
Available online 25 March 2019

quadruplex has been implicated in numerous biological processes, most of them only focus on intramolecular monomorphic G-quadruplex structures, and rarely on intermolecular parallel G-quadruplex, which are the essential features for the design of three-dimensional molecular scaffolds to detect MP in this work.

Graphene oxide (GO) possesses high water dispersibility, excellent surface-to-volume ratio, facile synthesis procedures, superb colloidal stability, strong absorptive capacity and marvelous biocompatibility [22–25], and can absorb single stranded DNA (ssDNA) via the interactions, such as π-π stacking, hydrogen bonding, hydrophobic interactions and van der Waals forces [26,27], while double stranded DNA (dsDNA) displays lower affinities because of the electrostatic repulsion when nucleobases are shielded by the negatively charged dsDNA phosphate backbone [28]. Moreover, it can efficiently quench the fluorescence of dyes through fluorescence resonance energy transfer (FRET), has thus been used as a versatile candidate for detection of biomarkers [29–31], pathogenic agents [32], oligonucleotides [33] and many other small molecules [34]. Here the interaction of TP-G4 with GO induced the adsorption of TP-G4 on GO surface and thus quenched the fluorescence of dye molecules labeled to TP-G4. The designed probe showed specific recognition to target DNA to quickly release the TP-G4, leading to a new sensitive "signal-on" fluorescence biosensing platform. The convenient operation, quick response, and high sensitivity for the detection of MP meet the demands of early point-of-care testing. The biosensing platform is versatile and can be used for different DNA analytes by changing the sequence of parallel strands, showing its promising application in clinic diagnosis.

2. Experimental section

2.1. Materials and reagents

Tris(hydroxymethyl) aminomethane (Tris), KCl and $MgCl_2$ were obtained from Sigma-Aldrich (St. Louis, MO, USA). Graphene oxide (GO) was purchased from Nanjing XFNANO Materials Tech. Co., Ltd (Nanjing, China), with diameter of 0.5–5 μm, thickness of 0.8–1.2 nm and single layer of more than 99%. Nucleic acid gel loading buffer was acquired from Thermo Fisher Scientific. Co., Ltd. (Shanghai, China). UltraPower™ DNA dye was acquired from Bio Teke. Co., Ltd. (Beijing, China). Human saliva samples were collected from The Second Affiliated Hospital of Hainan Medical University. All oligonucleotides were dissolved in 10 mM Tris-HCl (pH 7.4, containing 150 mM KCl, 10 mM $MgCl_2$). Ultrapure water obtained from the Millipore water purification system (electric resistivity ≥18 MΩ.cm, Milli-Q, Millipore) was used in all assays. All of the reagents were of analytical grade and used without further purification.

All DNA strands were synthesized and purified in HPLC by Shanghai Sangon Biotechnology Co. Ltd. (Shanghai, China). Some of them were labeled with 6-carboxyfluorescein (FAM). Their sequences are listed as follows (from 5′ to 3′):

G4-P: GGGGCACTCGGTTAACCTCCATTATGTT-FAM
G5-P: GGGGGCACTCGGTTAACCTCCATTATGTT-FAM
G6-P: GGGGGGCACTCGGTTAACCTCCATTATGTT-FAM
G0-P: CACTCGGTTAACCTCCATTATGTT—FAM
GT4G-P: GTTTTGCACTCGGTTAACCTCCATTATGTT
6 G: GGGGGG-FAM
MP target: AACATAATGGAGGTTAACCGAGTG
Mis-1 (M1): AACATAATGGAGGTTAACAGAGTG
Mis-3 (M3): AACATATTGGAGCTTAAGCGAGTG
Random (R): TTAGTGTGACTGATGAGTCTATGT
Legionella pneumophila target (LP): AGTGAATTTTGCAGAGATGC ATTA
Chlamidophila pneumoniae target (CP): TAGAAATACAGCTTTCCG CAAGGA
Streptococcus pneumoniae target (SP): GAGTTTTCCTTCGGGACAG AGGTG

The design of the target DNA was mainly based on the 16 s rRNA gene sequence of mycoplasma pneumoniae M129 (GenBank: U00089.2). The specificity of the target DNA sequence was corroborated by blast alignment from the National Center for Biotechnology Information (NCBI, USA) [35].

2.2. Apparatus

Fluorescence spectra were recorded on F-7000 fluorescence spectrophotometer (HITACHI, Japan). The ultraviolet-visible (UV–vis) absorption spectra were measured on a Cary 100 UV–vis spectrophotometer (Agilent). Polyacrylamide gel electrophoresis (PAGE) analysis was performed on an electrophoresis analyser (Bio-Rad, USA) and imaged on Bio-rad ChemDoc XRS (Bio-Rad, USA). CD spectra were measured on a Chirascan circular dichroism spectropolarimeter (Applied Photophysis). Ultrasonic dispersion was performed on an ultrasonic cell grinder (Shangjia Bio-Tech, China).

2.3. Preparation of GO solution and G-quadruplex structure

10 mg graphene oxide sheet was dispersed into 10 mL of deionized water, then placed in ultrasonic cell grinder, where ultrasonic dispersion was exposed in an ice bath at 300 W, stirring every 30 min for 3 h before a homogeneous brownish yellow GO solution was obtained. The final concentration of GO solution was 1 mg/mL, which was placed at room temperature for further experiments.

To obtain the tetramolecular G-quadruplex, DNA stock solution was prepared in 10 mM Tris-HCl (pH 7.4, containing 150 mM KCl, 10 mM $MgCl_2$) at 200 μM, which was denatured at 95 °C for 5 min, cooled gradually to room temperature, and then stored at least one week at 4 °C for later use [11,17].

2.4. Gel electrophoresis and CD analysis

To verify the formation of the tetramolecular G-quadruplex structure, a 12% native PAGE in 1 × TBE running buffer was performed, and 7 μL of DNA samples and 1.5 μL of 6 × loading buffer were fully mixed for 3 min to ensure the combination before injection. After 90-min running on an electrophresis analyser at 110 V, the gel was stained with UltraPower™ DNA dye for 20 min and then exposed under UV light and photographed with a Molecular Imager Gel Doc XR.

The CD data were collected from 220 nm to 350 nm at room temperature. The DNA samples were dissolved in Tris-HCl and the final concentration was 5 μM.

2.5. Fluorescent DNA assay

In brief, 8 μL of 5 μM G-quadruplex was mixed with 4.8 μL of 675 μg/mL GO in 179.2 μL of 10 mM Tris-HCl buffer for 3 min. Afterwards, different concentrations of target DNA (from 0 μM to 10 μM) in the same volume of 8 μL were added to the reaction solution to hybrid at room temperature for 10 min, and the fluorescence spectra were recorded from 505 nm to 650 nm at an excitation wavelength of 492 nm. The fluorescence intensity was measured at 525 nm.

3. Results and discussion

3.1. Design of sensing strategy

Scheme 1 illustrates the principle of the proposed strategy for MP detection using parallel-stranded TP as a three-dimensional molecular scaffold. The 5′ end of four DNA strands formed an intermolecular G-quadruplex, while the FAM labeled 3′ ends were single strands, which were completely complementary to the target MP. In the absence of target MP, the single-stranded 3′ ends could strongly interact with the surface of GO, which induced the adsorption of the G-quadruplex on

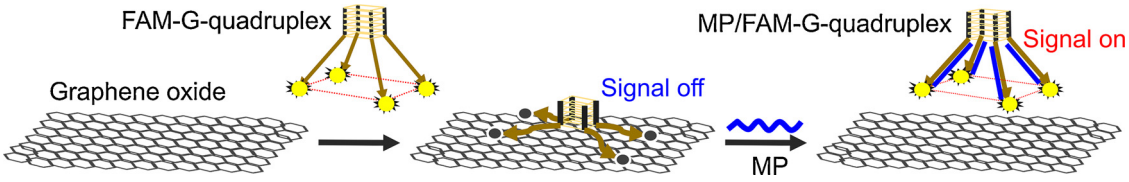

Scheme 1. Schematic representation of fluorescence detection of target MP based on the interaction of G-quadruplex and graphene oxide.

GO, and quenched the fluorescence of FAM by FRET. Upon the addition of target MP, the single-stranded 3′ ends hybridized with MP DNA to release the G-quadruplex from GO surface and thus restore the fluorescence of FAM. The fluorescence intensity depended on the MP concentration.

3.2. Formation of tetramolecular G-quadruplex

G-quadruplexes are generally divided two basic types: parallel and antiparallel, and the CD spectrum of parallel G-quadruplex has a positive peak around 264 nm and a negative peak around 240 nm, whereas the CD spectrum of antiparallel G-quadruplex has a positive peak around 290 nm and a negative peak around 260 nm [14]. Different from the CD spectrum of G0-P, which could not form G-quadruplex structure and showed the characteristic positive peak of single-stranded DNA at 280 nm, the CD spectra of G4-P, G5-P and G6-P showed the positive peaks at 270 nm and negative peaks at 240 nm (Fig. 1A). All the positive peaks deviated from both 264 and 290 nm, which could be attributed to the presence of the single-stranded P oligonucleotide limbs. After subtracting the contribution of single-stranded DNA of G0-P to the CD spectra, the positive peaks of G4-P, G5-P and G6-P shifted to 264 nm, and were consistent with the peak position of 6 G, a control to form parallel G-quadruplex structure without the limbs, indicating the formation of parallel tetrapod G-quadruplex structure [36]. Furthermore, the presence of continuous G groups was necessary for forming the parallel G-quadruplex structure, which was demonstrated by the CD spectrum of GT4G-P. The absolute peak intensity related to tetrapod G-quadruplex gradually increased with the increasing number of G nucleotides from 4 to 6.

The formation of parallel tetrapod G-quadruplex structure was further demonstrated with electrophoresis analysis. As shown in Fig. 1B, GT4G-P (lane 4) appeared only a single low-molecular weight band, and its migration was similar to those observed for G4-P, G5-P and G6-P (lanes 3, 2, 1), verifying the absence of the G-quadruplex structure. However, G4-P, G5-P and G6-P showed another high-molecular weight band due to the formation of the G-quadruplex structure, which led to brighter band for greater number of G bases.

3.3. Feasibility

To manifest the feasibility of this strategy, the fluorescence emission spectra of G6-P at different conditions were recorded (Fig. 2). G6-P showed a strong fluorescence emission peak due to the presence of FAM (Fig. 2A, curve a). The peak intensity greatly decreased upon addition of GO, which led to 90% fluorescence quenching (Fig. 2A, curve b), indicating the high fluorescence quenching efficiency of GO. The quenching could be finished in about 2 min (Fig. 2B), indicating the quick adsorption of G6-P on GO surface. By contraries, the fluorescence spectra of 6 G in the presence and absence of GO did not obviously change (Fig. 2C, D), indicating the lack of adsorption due to the electrostatic repulsion when nucleobases were shielded by the negatively charged phosphate backbone of 6 G (G-quadruplex DNA) [21]. The slight decrease in fluorescence intensity upon the addition of GO might be due to the presence of small amounts of the single-stranded oligonucleotides.

After 200 nM target MP was added to this system, 81% fluorescence recovery was observed (Fig. 2A, curve c), indicating the release of the G6-P from GO surface in the form of MP/G6-P complex due to the hybridization of the 3′ ends with MP DNA. The reaction rate was relatively quick, it could reach the maximum fluorescence recovery in about 10 min (Fig. 2B). It was worthwhile to point out that the recovery was over 60% of the total fluorescence in 1 min. The rapid recovery of fluorescent signal could be attributed to the mutual repulsion between the GO and the tetramer on the G6-P structure, which promoted the release of the formed MP/G6-P complex. Since a G6-P could theoretically hybridize with four MP DNA strands, the formation of MP/G6-P complex with two or three hybridization products further accelerated the release. Thus the designed strategy showed the fastest response in comparison with those of other sensors (Table 1), moreover, it also showed better performance in linear range [24,33,37] and detection limit [24,36].

3.4. Optimization of GO amount and G nucleotide number

The amount of GO was a crucial factor for the effective detection of target MP. Low concentration of GO could not provide sufficient binding sites for the adsorption of G6-P, resulting in low quenching efficiency. Thus, the fluorescence intensity decreased with the increasing amount of added GO (Fig. 3), which reached a plateau at 15 μg/mL, signifying that all G6-P was attached to the surface of GO.

The thermodynamic stability of parallel G-quadruplex increases with the increase of G number (from 3 to 8 G) and reaches a plateau for 6 G, which was demonstrated with CD, melting temperature and H NMR measurements [11]. The PAGE analysis showed that the bands

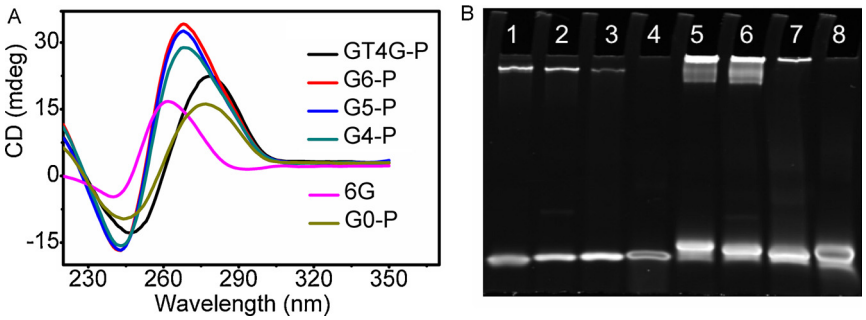

Fig. 1. (A) CD spectra of 5 μM G6-P, G5-P, G4-P, GT4G-P, G0-P and 6 G. (B) PAGE of 2.5 μM G6-P (1), G5-P (2), G4-P(3), GT4G-P (4), and the mixture of 2.5 μM MP DNA and 2.5 μM G6-P (5), G5-P(6), G4-P (7) and GT4G-P (8).

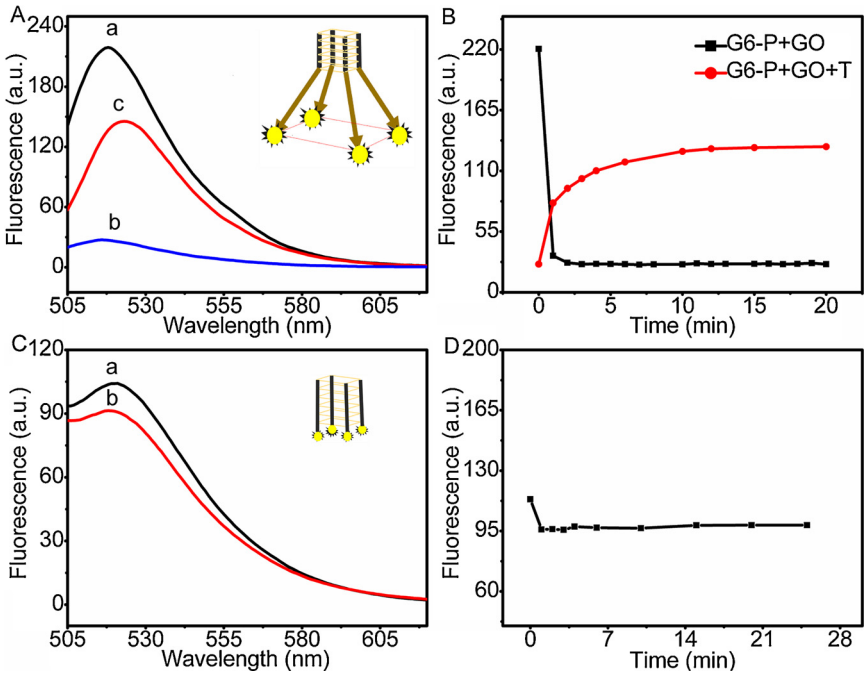

Fig. 2. (A) Fluorescence emission spectra of (a) 200 nM G6-P, (b) (a) + 15 μg/mL GO, and (c) (b) + 250 nM MP. (B) Fluorescence intensity of 200 nM G6-P + 15 μg/mL GO in absence and presence of 200 nM target MP as a funtion of time. (C) Fluorescence emission spectra of 200 nM 6 G before and after addition of 15 μg/mL GO. (D) Fluorescence intensity of 200 nM 6 G + 15 μg/mL GO as a function of time.

Table 1
Comparison of methods for fluorescence detection of short DNA or RNA based on GO.

DNA probe	Assay time	Linear range	LOD	Ref.
Molecular beacon	1 h	5-500 nM	2.0 nM	[36]
ssDNA	30 min	–	–	[25]
Graphene quantum dots	30 min	6.7-46.0 nM	75.0 pM	[33]
ssDNA	30 min	50-200 nM	–	[37]
AIE molecule	Less than 30 min	5-100 nM	2.5 nM	[24]
G-quadruplex	10 min	5-300 nM	3.96 nM	This work

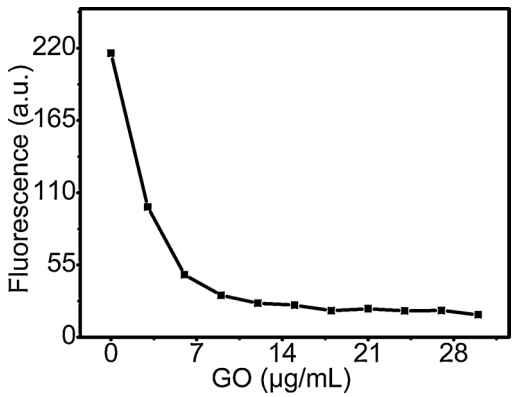

Fig. 3. Fluorescence intensity of 200 nM G6-P in the presence of different concentrations of GO.

with higher molecular weight occurred after the addition of MP DNA to the G-quadruplex solutions, indicating their hybridization due to the presence of single-stranded 3′ end (Fig. 1B, lanes 7, 6, 5). Moreover, the band turned brighter as the number of G bases increased. After MP DNA was added to G-quadruplex/GO solutions, the fluorescence recovery efficiency (F/F_0) increased from 4 to 6 G (Fig. 4), which might be due to both the greater mutual repulsion between the GO and the tetramer on the G6-P structure, and the relatively good thermodynamic stability of G6-P.

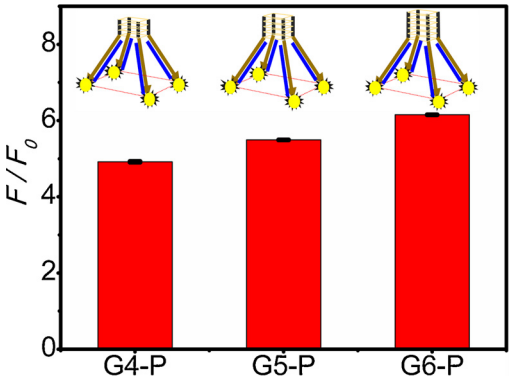

Fig. 4. F/F_0 values for G4-P/GO, G5-P/GO and G6-P/GO upon addition of MP for 10 min. The error bars represent the standard deviation of three independent measurements.

3.5. Sensitivity and selectivity

Under the optimal conditions, the detection capability of the biosensing platform based on the interaction of G6-P with GO was studied from the sensitivity and selectivity. The fluorescence intensity increased with the increasing MP concentration (Fig. 5A). The plot of the fluorescence intensity *vs* the concentration of MP showed a good linear relationship in the range of 5–300 nM (Fig. 5B), and the linear regression equation was $F = 20.48 + 0.49 \times c$ ($R^2 = 0.998$), where F was the fluorescence intensity and c was MP concentration. The limit of detection was estimated to be 3.96 nM at 3σ. This sensitivity could meet the demand of clinical samples, since only a certain amount of MP can cause disease.

In order to investigate the selectivity of the proposed biosensing platform, the target MP (T), single-base mismatched target (M1), three-base mismatched target (M3) and non-complementary random sequence (R) were measured. As excepted, the fluorescence intensity of T was higher than M1, M3 and R, and the fluorescence intensity changes (F/F_0) for T, M1, M3 and R were 6.06, 4.77, 3.43 and 1.27 times of that for the blank, respectively, where F_0 and F is the fluorescence intensity of G6-P/GO before and after target was added for 10 min, respectively. The change of fluorescence intensity for R was almost negligible

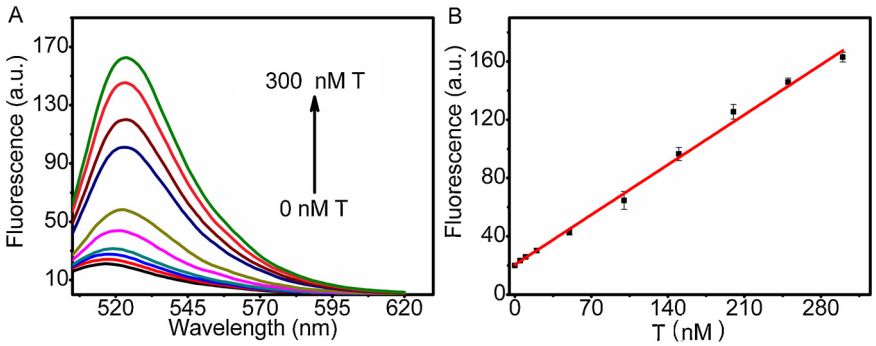

Fig. 5. (A) Fluorescence spectra of FAM-labeled G6-P/GO after adding 0, 5, 10, 20, 50, 100, 150, 200, 250 and 300 nM MP for 10 min. (B) Calibration curve. The error bars represent the standard deviation of three independent measurements.

Table 2
Determination of target MP in diluted saliva sample with the proposed method.

Sample No.	Added (nM)	Founded (nM)	RSD (%) (n = 3)	Recovery (%)	Bias%
1	10	10.5	6.7	105.2	5.0
2	20	19.9	5.9	99.5	−0.5
3	100	92.6	2.5	92.6	−7.4
4	200	200.8	4.5	100.4	0.4
5	250	249.3	5.2	99.7	−0.2
6	300	290.2	0.9	96.7	−3.3

relative to the blank solution, while the fluorescence change for target MP was significantly different from those for both single-base and three-base mismatched targets. Due to the conservative nature of the target MP, at least three-base mismatched target could lead to two different diseases, thus the distinguish of different target sequences was acceptable for the practicability of the biosensing platform in clinic diagnosis.

3.6. Detection of practical samples

To evaluate the application of the proposed method in the actual samples, six clinical human saliva samples were spiked with MP solution for recovery experiments. The saliva samples were collected from The Second Affiliated Hospital of Hainan Medical University with written patient-informed consent, which was approved by the Ethics Committee of Hainan Medical University (approval 2018-030). Considering the matrix effect of real saliva samples, the cut-off value of MP for clinical diagnosis, the practical amount of MP in positive samples and the sensitivity of the proposed method, the saliva samples were diluted for 20 times with ultrapure water. As listed in Table 2, the recoveries were in the range from 92.6% to 105.2% with relative standard deviations of 0.9%–6.7% for three determinations. Meanwhile, the stability and selectivity of the sensor were also examined with the diluted saliva samples. The performance of the sensor was stable, and 92% of the original fluorescence could be remained after stored at 4 °C for five days (Fig. S1). When tested with LP, CP and SP each at the concentration of 200 nM, no obvious change in fluorescence intensity relative to the blank could be observed, while significant fluorescence enhancement occurred after the addition of 200 nM MP (Fig. S2). These results revealed that the proposed method could be used as an effective platform for the detection of target MP with a satisfactory accuracy in the actual saliva samples.

4. Conclusions

This work develops a fluorescence “signal-on” approach for fast detection of MP based on the interaction graphene oxide and the designed tetrapod G-quadruplex. The tetramolecular G-quadruplex can be conveniently formed with G_n-P (n = 4–6). The presence of single-stranded P makes the G-quadruplex be quickly adsorbed on GO surface to quench the fluorescence of FAM labelled to 3′ end of P. The hybridization of the P with MP DNA leads to rapid release of the G-quadruplex from GO to restore the fluorescence. The assay of target DNA is simple and fast, and can be performed in homogeneous system. The proposed method shows high sensitivity and acceptable distinguish of different target sequences. By changing the sequence of P, the convenient assay can be used as a versatile method to detect other DNA analytes.

Acknowledgements

We gratefully acknowledge the National Natural Science Foundation of China (81860373, 81460306 and 31160030), and the Finance Science and Technology Project of Hainan Province (ZDXM2014069).

Appendix A. Supplementary data

Supplementary material related to this article can be found, in the online version, at doi:https://doi.org/10.1016/j.snb.2019.03.103.

References

[1] M. Carrim, N. Wolter, A.J. Benitez, S. Tempia, M. du Plessis, S. Walaza, et al., Epidemiology and molecular identification and characterization of mycoplasma pneumoniae, Emerg. Infect. Dis. 24 (2018) 506–513.
[2] R. Himmelreich, H. Hilbert, H. Plagens, E. Pirkl, B.C. Li, R. Herrmann, Complete sequence analysis of the genome of the bacterium mycoplasma pneumoniae, Nucleic Acids Res. 24 (1996) 4420–4449.
[3] T.P. Atkinson, M.F. Balish, K.B. Waites, Epidemiology, clinical manifestations, pathogenesis and laboratory detection of mycoplasma pneumoniae infections, FEMS Microbiol. Rev. 32 (2008) 956–973.
[4] T.N. Canavan, E.F. Mathes, I. Frieden, K. Shinkai, Mycoplasma pneumoniae–induced rash and mucositis as a syndrome distinct from Stevens-Johnson syndrome and erythema multiforme: a systematic review, J. Am. Acad. Dermatol. 72 (2015) 239–245.
[5] L.G. Smith, Mycoplasma pneumonia and its complications, Infect. Dis. Clin. North Am. 24 (2010) 57–60.
[6] K.B. Waites, D.F. Talkington, Mycoplasma pneumoniae and its role as a human pathogen, Clin. Microbiol. Rev. 17 (2004) 697–728.
[7] G.L. Parrott, T. Kinjo, J. Fujita, A compendium for mycoplasma pneumoniae, Front. Microbiol. 7 (2016) 513.
[8] K.B. Waites, L. Xiao, Y. Liu, M.F. Balish, T.P. Atkinson, Mycoplasma pneumoniae from the respiratory tract and beyond, Clin. Microbiol. Rev. 30 (2017) 747–809.
[9] K. Loens, M. Ieven, Mycoplasma pneumoniae: current knowledge on nucleic acid amplification techniques and serological diagnostics, Front. Microbiol. 7 (2016) 448.
[10] D. Sen, W. Gilbert, A sodium-potassium switch in the formation of four-stranded G4-DNA, Nature 344 (1990) 410–414.
[11] L. Zhu, J. Zhou, G. Xu, C. Li, P. Ling, B. Liu, et al., DNA quadruplexes as molecular scaffolds for controlled assembly of fluorogens with aggregation-induced emission, Chem. Sci. 9 (2018) 2559–2566.
[12] C. Bardin, J.L. Leroy, The formation pathway of tetramolecular G-quadruplexes, Nucleic Acids Res. 36 (2008) 477–488.
[13] F. He, Y. Tang, S. Wang, Y. Li, D. Zhu, Fluorescent amplifying recognition for DNA

G-quadruplex folding with a cationic conjugated polymer: a platform for homogeneous potassium detection, J. Am. Chem. Soc. 127 (2005) 12343–12346.
[14] J. Kypr, I. Kejnovska, D. Renciuk, M. Vorlickova, Circular dichroism and conformational polymorphism of DNA, Nucleic Acids Res. 37 (2009) 1713–1725.
[15] J.L. Huppert, Four-stranded nucleic acids: structure, function and targeting of G-quadruplexes, Chem. Soc. Rev. 37 (2008) 1375–1384.
[16] S. Burge, G.N. Parkinson, P. Hazel, A.K. Todd, S. Neidle, Quadruplex DNA: sequence, topology and structure, Nucleic Acids Res. 34 (2006) 5402–5415.
[17] Y. Guo, J. Chen, M. Cheng, D. Monchaud, J. Zhou, H. Ju, A thermophilic tetramolecular G-quadruplex/hemin DNAzyme, Angew. Chem. Int. Ed. 56 (2017) 16636–16640.
[18] G. Pelossof, R. Tel-Vered, I. Willner, Amplified surface plasmon resonance and electrochemical detection of Pb^{2+} ions using the Pb^{2+}-dependent DNAzyme and hemin/G-quadruplex as a label, Anal. Chem. 84 (2012) 3703–3709.
[19] D. Yang, X. Liu, Y. Zhou, L. Luo, J. Zhang, A. Huang, et al., Aptamer-based biosensors for detection of lead(ii) ion: a review, Anal. Methods 9 (2017) 1976–1990.
[20] C. Zhao, L. Wu, J. Ren, X. Qu, A label-free fluorescent turn-on enzymatic amplification assay for DNA detection using ligand-responsive G-quadruplex formation, Chem. Commun. 47 (2011) 5461–5463.
[21] Y. Shi, W.T. Huang, H.Q. Luo, N.B. Li, A label-free DNA reduced graphene oxide-based fluorescent sensor for highly sensitive and selective detection of hemin, Chem. Commun. 47 (2011) 4676–4678.
[22] M.A. Worsley, P.J. Pauzauskie, T.Y. Olson, J. Biener, J.H. Satcher, T.F. Baumann, Synthesis of graphene aerogel with high electrical conductivity, J. Am. Chem. Soc. 132 (2010) 14067–14069.
[23] H.Y. Choi, T.J. Lee, G.M. Yang, J. Oh, J. Won, J. Han, et al., Efficient mRNA delivery with graphene oxide-polyethylenimine for generation of footprint-free human induced pluripotent stem cells, J. Control. Release 235 (2016) 222–235.
[24] A. Tyagi, K.L. Chu, I.H. Abidi, A.A. Cagang, Q. Zhang, N.L.C. Leung, et al., Single-probe multistate detection of DNA via aggregation-induced emission on a graphene oxide platform, Acta Biomater. 50 (2017) 334–343.
[25] C. Lu, Hua hyphen, H. Yang, Hao hyphen, et al., A graphene platform for sensing biomolecules, Angew. Chem. Int. Ed. 121 (2009) 4879–4881.
[26] Y. Xu, Q. Wu, Y. Sun, H. Bai, G. Shi, Three-dimensional self-assembly of graphene oxide and DNA into multifunctional hydrogels, ACS Nano 4 (2010) 7358–7362.
[27] Z. Tang, H. Wu, J.R. Cort, G.W. Buchko, Y. Zhang, Y. Shao, et al., Constraint of DNA on functionalized graphene improves its biostability and specificity, Small 6 (2010) 1205–1209.
[28] L. Cui, X. Lin, N. Lin, Y. Song, Z. Zhu, X. Chen, et al., Graphene oxide-protected DNA probes for multiplex microRNA analysis in complex biological samples based on a cyclic enzymatic amplification method, Chem. Commun. 48 (2012) 194–196.
[29] Q. Wu, B. Jiang, Y. Weng, J. Liu, S. Li, Y. Hu, et al., 3-Carboxybenzoboroxole functionalized polyethylenimine modified magnetic graphene oxide nanocomposites for human plasma glycoproteins enrichment under physiological conditions, Anal. Chem. 90 (2018) 2671–2677.
[30] C. Zhang, Y. Yuan, S. Zhang, Y. Wang, Z. Liu, Biosensing platform based on fluorescence resonance energy transfer from upconverting nanocrystals to graphene oxide, Angew. Chem. Int. Ed. 50 (2011) 6851–6854.
[31] S. He, B. Song, D. Li, C. Zhu, W. Qi, Y. Wen, et al., A graphene nanoprobe for rapid, sensitive, and multicolor fluorescent dna analysis, Adv. Funct. Mater. 20 (2010) 453–459.
[32] J.H. Jung, D.S. Cheon, F. Liu, K.B. Lee, T.S. Seo, A graphene oxide based immunobiosensor for pathogen detection, Angew. Chem. Int. Ed. 49 (2010) 5708–5711.
[33] Z.S. Qian, X.Y. Shan, L.J. Chai, J.J. Ma, J.R. Chen, H. Feng, A universal fluorescence sensing strategy based on biocompatible graphene quantum dots and graphene oxide for the detection of DNA, Nanoscale 6 (2014) 5671–5674.
[34] F. Li, Y. Feng, C. Zhao, P. Li, B. Tang, A sensitive graphene oxide–DNA based sensing platform for fluorescence “turn-on” detection of bleomycin, Chem. Commun. 48 (2012) 127–129.
[35] S. Yu, Y. Tang, M. Yan, Z.P. Aguilar, W. Lai, H. Xu, A fluorescent cascade amplification method for sensitive detection of Salmonella based on magnetic Fe_3O_4 nanoparticles and hybridization chain reaction, Sens. Actuators B Chem. 279 (2019) 31–37.
[36] C.H. Lu, J. Li, J.J. Liu, H.H. Yang, X. Chen, G.N. Chen, Increasing the sensitivity and single-base mismatch selectivity of the molecular beacon using graphene oxide as the "nanoquencher", Chem. Eur. J. 16 (2010) 4889–4894.
[37] Z. Lu, L. Zhang, Y. Deng, S. Li, N. He, Graphene oxide for rapid microRNA detection, Nanoscale 4 (2012) 5840–5842.